

Lawrence Berkeley National Laboratory

LBL Publications

Title

Characterization of a gamma-ray tracking array: A comparison of GRETINA and Gammasphere using a ^{60}Co source

Permalink

<https://escholarship.org/uc/item/7wb5k8h5>

Authors

Lauritsen, T

Korichi, A

Zhu, S

et al.

Publication Date

2016-11-01

DOI

10.1016/j.nima.2016.07.027

Peer reviewed

Characterization of gamma-ray tracking arrays: a comparison of GRETINA and Gammasphere using a ^{60}Co source

T. Lauritsen^a, A. Korichi^b, S. Zhu^a, A.N. Wilson^c, D. Weisshaar^d, J. Dudouet^e, A.D. Ayangeakaa^a, M.P. Carpenter^a,
C.M. Campbell^f, E. Clement^h, H.L. Crawford^f, M. Cromaz^f, P. Fallon^f, J.P. Greene^a, R.V.F. Janssens^a, T.L. Khoo^a, N. Lalović^{k,i},
I.Y. Lee^f, A.O. Macchiavelli^f, R.M. Perez-Vidal^g, S. Pietriⁱ, D.C. Radford^j, D. Ralet^b, L. Riley^l, D. Seweryniak^a, O. Stezowski^e

^aArgonne National Laboratory, Argonne, Illinois 60439, USA

^bC.S.N.S.M, IN2P3-CNRS, bat 104-108, F-91405 Orsay Campus, France

^cUniversity of the West of Scotland, Paisley, UK

^dNSCL, Michigan state University, USA

^eI.P.N. Lyon, IN2P3-CNRS, Lyon Campus, France

^fLawrence Berkeley National Laboratory, Berkeley, CA 94720, USA

^gInstituto de Fisica Corpuscular, CSIC-Universitat de Valencia, E-46920 Valencia, Spain

^hGANIL, CEA/DSM-CNRS/IN2P3, BP 55027, F-14076 Caen, France

ⁱGSI Helmholtzzentrum für Schwerionenforschung GmbH, D-64291 Darmstadt, Germany

^jPhysics Division, Oak Ridge National Laboratory, Oak Ridge, Tennessee 37831, USA

^kDepartment of Physics, Lund University, SE-22100 Lund, Sweden

^lUrsinus College, Collegetown, PA 19426, USA

Abstract

In this paper, we provide a formalism for the characterization of the tracking arrays with emphasis on the proper corrections required to extract their photopeak efficiencies and peak-to-total ratios. The methods are first applied to Gammasphere, a well characterized 4π array based on the principle of Compton suppression, and subsequently to GRETINA. The tracking efficiencies are then discussed and some guidelines as to what clustering angle to use in the tracking algorithm are presented. It was possible, using GEANT4 simulations, to scale the measured efficiencies up to the expected values for the full 4π implementation of GRETA.

Keywords: Segmented germanium detectors, efficiency measurements, γ -ray tracking, Gammasphere, GRETINA, GRETA, γ -ray spectroscopy, nuclear structure.

Contents

Contents		4.2 The efficiency of GRETINA at ANL	7
1 Introduction	2	4.3 The efficiency of GRETINA at MSU	8
2 Efficiency and peak-to-total ratio measurements	2	4.4 Angular correlations in tracking arrays	8
2.1 The peak areas in a ^{60}Co source spectrum	3	4.5 Comparing ^{60}Co source spectra	9
2.2 The efficiencies, true counts and (P/T) ratios	4	4.6 Comparing the (P/T) ratios versus the efficiency curves for GRETINA	9
2.3 The external trigger method	4	5 Discussion	9
3 Tracking	5	6 Conclusions and outlook	11
3.1 The tracking efficiency	5	7 Acknowledgments	12
3.2 The clustering angle (α)	6	Appendix A Deadtime and random rates	12
4 Results and comparisons	7	Appendix A.1 Deadtimes in Gammasphere	12
4.1 The efficiency of Gammasphere	7	Appendix A.2 Deadtimes in tracking arrays	12

Email address: torben@anl.gov (T. Lauritsen)

1 **1. Introduction**

2 The concept of escape suppression revolutionized the field of γ -
3 ray spectroscopy, enabling significant increases in the resolving
4 power of germanium-based detector arrays [1–3]. Now, the new
5 concept of γ -ray tracking and recent advances in germanium
6 (Ge) crystal segmentation technology are leading to another
7 revolution where escape suppression shields are removed and
8 only Ge crystals are used, filling as much of the space around
9 the source of γ rays as possible [4].

10 The tracking concept is based on the ability to locate, within a
11 few mm, each photon interaction point in the Ge detector and,
12 consequently, to track the scattering sequence of an incident
13 photon through the crystals. The method consists in the recon-
14 struction of the full γ -ray energy by combining the appropriate
15 interaction points [5–9].

16 This approach provides a significant gain in detection efficiency
17 over escape-suppressed arrays because the Compton suppres-
18 sion shields (which limit the Ge solid angle) are removed and
19 replaced by active Ge detectors. For the first time, a nearly
20 4π sphere of Ge, with a good peak-to-total ratio, becomes
21 possible. Moreover, the tracking technique provides identifica-
22 tion of the first interaction point with good angular resolu-
23 tion and, therefore, allows for an improved Doppler correc-
24 tion. The expected performance for tracking detector arrays
25 are thus well beyond those of escape-suppressed spectrom-
26 eters like EUROBALL [10] and Gammasphere [11, 12]. The
27 most advanced implementations of this concept to date are the
28 two arrays AGATA (Advanced GAMMA Tracking Array) [13]
29 and GRETINA (Gamma Ray Energy Tracking In beam Nu-
30 clear Array) [14]. GRETINA is the early implementation of
31 GRETA (Gamma Ray Energy Tracking Array) [15]. These
32 arrays are built from large, segmented crystals of hyper-pure
33 germanium (HPGe) and are the first to use the concept of
34 γ -ray energy tracking. This technique enables experiments
35 probing low cross sections and/or measurements using high-
36 velocity reaction products like those possible with stable and
37 radioactive beams at new facilities such as SPIRAL2 [16],
38 SPES [17], GANIL [18] and FAIR[19] in Europe and AT-
39 LAS/CARIBU [20], NSCL [21] and FRIB [22] in the USA.

40 The resolving power of a γ -ray detector array (*i.e.*, its abil-
41 ity to isolate a given sequence of γ rays in a complex spec-
42 trum) depends on four main properties [23]: efficiency, energy
43 resolution, peak-to-total ratio (P/T) (the ratio of photopeak
44 efficiency to the total efficiency [24]), and granularity. The
45 GRETINA array, and the future 4π array GRETA, are being de-
46 signed to maximize each of these properties. As these new sys-
47 tems begin to be used in experimental campaigns, it is important
48 that their performances be evaluated accurately. While Monte
49 Carlo simulations using GEANT4 can be used to some extent
50 for this purpose, simulations require precise knowledge of all
51 the detector parameters, such as geometry, mounting hardware

54 However, measurements – particularly those related to effi-
55 ciency calibrations – represent a challenge for tracking arrays,
56 and need to be fully understood and carried out carefully. Both
57 the efficiency and (P/T) depend on parameters that determine
58 whether a tracking algorithm associates a set of interaction
59 points with a single γ ray, multiple γ rays, or a scattered γ ray
60 with partial energy collection. Thus, no single, absolute value
61 of either quantity can be measured. Instead, one must examine
62 the correlation between efficiency and (P/T) in order to find
63 conditions that optimize both.

64 This paper describes possible ways to determine array efficien-
65 cies, with an emphasis on the proper corrections, and explores
66 how different methods compare. We use a ^{60}Co source to ob-
67 tain efficiencies at 1333 keV; because this is a multiplicity two
68 source (*i.e.*, it emits two γ rays), we also investigate the required
69 correction terms. First, we describe in detail the different meth-
70 ods proposed. Each approach is then validated using data from
71 a well-understood, Compton-suppressed 4π array: Gammas-
72 phere. The approaches are then applied to data obtained with
73 GRETINA in two geometries, one at Argonne National Labora-
74 tory (ANL) and one at Michigan State University (MSU). At the
75 time of the measurements, the Gammasphere array consisted of
76 95 escape-suppressed Ge detectors; the results reported below
77 have, therefore, been scaled to provide the characteristics of the
78 more standard 100 detector set-up. GRETINA was comprised
79 of seven quad modules (28 crystals) in compact setups at its
80 nominal distance (18.5 cm from the center position of the array
81 to the front of the Ge crystals) [14]. The results for the track-
82 ing array is then scaled to the future full 4π implementation
83 (GRETA) in order to compare the performance with Gammas-
84 phere.

2 **2. Efficiency and peak-to-total ratio measurements**

The photopeak efficiency, ϵ_p , is defined as the probability that a
single emitted γ ray is measured in the photopeak in the spec-
trum. The total efficiency, ϵ_T , is defined as the probability that
a γ ray adds one or more counts anywhere in the spectrum. The
ratio of these efficiencies is known as the (P/T) ratio. In the fol-
lowing, we describe our approaches to obtaining the photopeak
efficiency and (P/T) ratio from ^{60}Co source spectra. For this
source, the efficiency is traditionally reported for the 1333-keV
transition.

We chose the ^{60}Co source both because it is commonly used
for such measurements and because it allows efficiencies to
be obtained using both the so-called calibrated source (CSM)
and sum peak (SPM) methods [25–28]. Each of these two ap-
proaches can be applied to spectra generated from a given array
in different ways. For both conventional and tracking arrays,
two spectra can be created using the signals from the central
contacts (CC) of the Ge detectors. One, henceforth referred

to as CCsum, is created by producing spectra for each individual detector and subsequently adding these together. The other, referred to as CCcal below, is a calorimetric spectrum obtained by adding up the energies from all central contacts and histogramming these into one single spectrum. Whichever method is used, it is important to apply the proper corrections when extracting peak areas, taking into account all effects such as: one γ ray removes counts in the other one (in the case of a ^{60}Co source) and/or the effect of having random background γ rays in addition to the γ rays from the source [26, 27]. These considerations are described in sections 2.1 and 2.2.

A third way of obtaining the efficiency at 1333 keV for a ^{60}Co source consists of employing either an additional detector outside the array to trigger on the detection of the coincident 1173-keV transition, or in using an internal detector in the array in the same manner. These methods are described in Sec. 2.3.

While these approaches can be applied to both conventional and tracking arrays, the latter are designed to produce tracked spectra and this requires further processing of the data. The additional factors required to take into account the tracking efficiency are presented in section 3.1.

2.1. The peak areas in a ^{60}Co source spectrum

The CSM relies on a measurement of the observed area of the 1333-keV peak, taking into account a number of corrections, and knowledge of the source strength. The SPM relies on the precise determination of the areas of all three of the 1173-, 1333- and (sum) 2506-keV peaks in the ^{60}Co source spectrum. In either case, the peak areas depend on several factors, including the efficiencies at both 1173 and 1333 keV. In fact, the observed areas of the three peaks in a ^{60}Co source spectrum can be written as:

$$A^{obs}(1173) = S \epsilon_p(1173)(1 - C_k(1333)) \times (1 - C_R)(1 - C_s(1173)), \quad (1)$$

$$A^{obs}(1333) = S \epsilon_p(1333)(1 - C_k(1173)) \times (1 - C_R)(1 - C_s(1333)), \quad (2)$$

$$A^{obs}(2506) = \frac{1}{N} S \epsilon_p(1173) \epsilon_p(1333) C_f(1 - C_R) \times (1 - C_s(1173))(1 - C_s(1333)), \quad (3)$$

where

$$C_k(e) = \frac{C_o C_f \epsilon_T(e)(1 + C_s(e))}{N}, \quad (5)$$

$$(P/T) \equiv \epsilon_p / \epsilon_T, \quad (6)$$

$$C_R = \frac{\epsilon_R \Delta t}{N} \frac{dR}{dt}, \quad (7)$$

$$S = A_S t L_F. \quad (8)$$

ϵ_T is the total array efficiency, ϵ_p the array photopeak efficiency and (P/T) is the peak-to-total ratio, all of which are energy dependent. N is the number of crystals in the array with $N \equiv 176$

for the calorimetric CCcal spectra and $N > 1$ for the CCsum spectra. S denotes the total number of γ rays emitted by the source (during the acquisition time t), corrected for any dead-time or loss in efficiency of the system through the live fraction (L_F) [24]. A_S is the source activity and C_f corrects for the angular correlation between the 1173- and 1333-keV lines in the ^{60}Co source [29, 30]. The small corrections for internal conversion and branching ratios for the γ rays from the ^{60}Co source are ignored in the formulas; they are of the order of 0.01%.

To be consistent, one should report the (P/T) ratio at an energy of 1333 keV like the efficiency. However, traditionally, the (P/T) for a ^{60}Co source is reported as

$$(P/T)_{composite} = \frac{A(1173) + A(1333)}{A_{tot}} \quad (9)$$

We shall use this composite (P/T) ratio here as well, but will argue that $A(2506)$ needs to be added to the numerator unless it is tracked data. This ratio can be made from observed areas, $(P/T)^{obs}$, or for the corrected areas of the peaks (see discussion in Sec. 2.2). The composite (P/T) ratio in Eq. 9 can be written as a weighted average of the energy dependent (P/T) values in Eq. 6, using information from a measured response function [30] or spectra gated on the 1173- and 1333-keV lines. For Gammasphere, it is found that

$$(P/T)(1173) = (P/T)_{composite} \times 1.02212 \quad (10)$$

$$(P/T)(1333) = (P/T)_{composite} / 1.02212 \quad (11)$$

The value of C_f depends on whether the CCsum or CCcal spectra are used as well as on the distance from the Ge crystals to the source. The nominal value of C_f is found to be 1.1111 at zero degrees [29]. For Gammasphere, taking into account the opening angle of the Ge detectors ($\pm 7.5^\circ$), the attenuated C_f value is determined to be 1.109 for CCsum [30]. For CCcal spectra in Gammasphere, because the array covers almost 4π , C_f is close to one. For GRETINA, at the nominal distance, the C_f values are specified in Table 1 (see further discussion in Sec. 4.4). Just using the crystal center positions, the C_f values are calculated to be 1.0076 for GRETINA for CCcal spectra; but measured values will be used in the calculations.

Table 1: The angular correlation factors, C_f , used in this work. The values for GRETINA, for the CCcal spectra, are obtained from measurements presented in Sec. 4.4. GRETINA and Gammasphere are abbreviated GS and GT, respectively, in this table.

	$C_f(\text{GS})$	$C_f(\text{GT}) (\text{ANL})$	$C_f(\text{GT}) (\text{MSU})$
CCsum	1.109	1.107	1.107
CCcal	1.0	1.007	1.013

The combined terms $C_k(e)$ in Eq. 1–2 correct for the fact that one of the γ rays from the ^{60}Co source may hit the detector and remove counts that should belong to the photopeak of the other transition. If only this effect is included, $C_o \equiv 1$ [30]. Setting $C_o > 1$ allows for corrections *beyond* what is already reflected in any decrease of the (P/T) ratio caused by scattered γ rays.

177 C_R is the correction for random γ rays hitting the detector in₂₁₁
 178 addition to photons from the ^{60}Co source. In Eq. 7, $\frac{dR}{dt}$ is the₂₁₂
 179 background rate, Δt the coincidence time window and ϵ_R the
 180 mean efficiency for total absorption of the random γ rays.

181 Finally, the C_s coefficient is the probability for a γ ray to scatter
 182 out of a crystal, to be detected by other crystals in the array and
 183 successfully sum up to the photopeak energy. The coefficient is,
 184 per definition, > 0 only for the CCsum spectra. Its value can be
 185 determined by comparing the counts in the photopeaks of the
 186 CCsum and CCcal spectra, taking into account the other cor-
 187 rection factors in eqs. 1–2 or, alternatively, from Eq. 20 from
 188 Sec. 2.2 below. For tracking arrays this coefficient is signifi-
 189 cant. On the other hand, for Gammasphere, where the BGO
 190 Compton suppressors largely prevent direct scattering between
 191 neighboring crystals, the coefficient is smaller.

192 The concept behind the C_s parameter is also known from com-
 193 posite HPGe detectors, such as Clover detectors, where the
 194 energies deposited by a γ ray scattering between crystals are
 195 added back and the gain in photopeak counts is measured by
 196 the add-back factor F [31]. Treating a tracking array as a single,
 197 composite detector, one can also assign an add-back factor F
 198 describing the gain in photopeak counts by adding up all crystal
 199 energies. The relationship between F and C_s is:

$$C_s = \frac{F - 1}{F} \quad (12)$$

200 The C_s factor allows for the use of the CCsum spectrum to de-
 201 termine the efficiency of tracking arrays, though, not independ-
 202 dently of the CCcal spectrum.

203 2.2. The efficiencies, true counts and (P/T) ratios

204 Eqs. 1–3 indicate how the observed peak areas relate to the ac-
 205 tual array efficiencies. Once the peak areas have been correctly
 206 determined, efficiencies, true peak areas and peak-to-total ra-
 207 tios can be extracted.

208 For the summed peak method (SPM), the efficiency is given by:

$$\epsilon_p(1333) = N \left\{ \frac{A^{obs}(2506)}{A^{obs}(1173)C_f} \right\} / \left\{ 1 - C_s(1333) + \frac{A^{obs}(2506)C_o(1 + C_s(1173))}{A^{obs}(1173)N(P/T)(1333)} \right\} \quad (13)$$

209 On the other hand, for the calibrated source method (CSM), the
 210 efficiency is given by:

$$\epsilon_p(1333) = \frac{A^{obs}(1333)}{S(1 - C_R)(1 - C_s(1333))} + \frac{C_o(1 + C_s(1173))A^{obs}(2506)}{NS((P/T)(1173))(1 - C_R)(1 - C_s(1173))(1 - C_s(1333))} \quad (14)$$

Combining eqs. 1–3, we find that the true, corrected counts in
 the peaks are given by:

$$A^{true}(1173) \equiv S\epsilon_p(1173) = \frac{A^{obs}(1173)}{(1 - C_k(1333))(1 - C_R)(1 - C_s(1173))}, \quad (15)$$

$$A^{true}(1333) \equiv S\epsilon_p(1333) = \frac{A^{obs}(1333)}{(1 - C_k(1173))(1 - C_R)(1 - C_s(1333))}, \quad (16)$$

$$A^{true}(2506) \equiv S\epsilon_p(1173)\epsilon_p(1333)C_f = \frac{A^{obs}(2506)}{(1 - C_R)(1 - C_s(1173))(1 - C_s(1333))}. \quad (17)$$

213 It follows that the true (P/T) ratio for the spectra is:

$$(P/T)^{true} = \frac{A^{true}(1173) + A^{true}(1333) + A^{true}(2506)}{A_{tot}^{true}}, \quad (19)$$

where A_{tot}^{true} is the total number of counts in the spectra up to
 just past the 2506-keV sum line and is related to the observed
 counts by:

$$A_{tot}^{obs} = A_{tot}^{true} + \frac{C_s}{(P/T)^{true}} (A^{true}(1173) + A^{true}(1333) + A^{true}(2506)) \quad (20)$$

214 For CCcal spectra, A_{tot}^{true} is simply A_{tot}^{obs} . Note that, for an ideal
 215 4π array, all the γ rays from a ^{60}Co source will be in the 2506-
 216 keV peak in the CCcal spectrum; Eq. 19 remains valid in this
 217 case.

218 For Compton-suppressed arrays, the composite (P/T) ratio is
 219 traditionally determined using the CCsum spectrum. This spec-
 220 trum is most relevant for the spectra used in γ -ray spectroscopy
 221 with Compton-suppressed arrays. For tracking arrays, where
 222 photons can scatter freely between the crystals, obtaining the
 223 (P/T) ratio for the array using the CCsum spectrum is possible,
 224 but the additional correction factors mean that the result is less
 225 precise.

226 The proper (P/T) ratio values to use in eqs. 1–3, in order to
 227 determine $\epsilon_T = \frac{\epsilon_p}{(P/T)}$ (see Eq. 6), are in fact the $(P/T)^{true}$ ra-
 228 tio from Eq. 19, not the observed values. Since $(P/T)^{true}$ is not
 229 known until the efficiency is found from Eq. 13 or Eq. 14, fol-
 230 lowed by eqs. 15–19, a simple iteration procedure is applied to
 231 find the $(P/T)^{true}$ value that reproduces itself.

232 2.3. The external trigger method

233 A third approach, using the CCcal spectrum, provides another
 234 way to measure the efficiency of an array. If a ^{60}Co source is
 235 placed at the target position and an external detector is used to
 236 detect the 1173-keV line, then the counts in the 1333-keV peak
 237 of the CCcal spectrum can be written as:

$$A^{obs}(1333) = A_{ext}^{obs}(1173) \times \epsilon_p(1333)C_f(1 - C_R) \quad (21)$$

where $A_{ext}^{obs}(1173)$ is the number of counts seen in the 1173-keV peak in the external detector. Using this method, it should be necessary to correct for random events in the coincidence time window and for angular correlation effects. It follows that:

$$\epsilon_p(1333) = \frac{A_{ext}^{obs}(1333)}{A_{ext}^{obs}(1173)C_f(1 - C_R)} \quad (22)$$

The external detector could be made part of the tracking array data acquisition system (DAQ). In that case, one can keep track of how many times a 1333-keV line is seen in the tracking array when the channel with the external detector has observed a photopeak absorption of 1173 keV. This ensures that a 1333-keV γ ray has indeed been emitted.

A variation of this method is to identify events in which the 1173-keV transition was detected in one of the array's crystals, and then exclude that specific crystal from the counts contributing to the CCcal spectrum. The exclusion of one crystal from the CCcal spectrum can be taken into account by adding a $\frac{N}{(N-1)}$ correction factor to Eq. 22, where N is the number of crystals.

3. Tracking

The previous sections lay out the procedures for obtaining the array's efficiency at 1333 keV and for measurements of the (P/T) ratio for two types of *untracked* spectra, CCsum and CCcal. These spectra enable direct comparisons between conventional, escape-suppressed and new-generation tracking arrays. However, we are ultimately interested in the sensitivity of the arrays when used in the tracking mode. In the following, both the tracking efficiency and the tracking *deficiency* are considered, and we argue that the latter is an important quantity to evaluate.

3.1. The tracking efficiency

In tracking arrays, the signals from the preamplifiers are digitized into signal traces of a few micro-seconds length at typically 100 MHz sampling. In the decomposition, or pulse shape analysis, traces from the segments of the crystals are analyzed and the interaction positions are inferred from fits that compare these traces with a basis data set. Tracking algorithms are then used to reconstruct the trajectories of the incident γ rays in order to determine their energy and direction. To accomplish this, the algorithms must group interaction points into those likely originating from a given γ ray and establish their scattering sequence (or order). Tracking algorithms can be divided into two classes: those based on back tracking [5] and those based on clustering and forward tracking [6]. The latter approach is used in this work.

For photon energies of interest (tens of keV to 20 MeV), the main physical processes that occur when a photon interacts in germanium are Compton scattering, Rayleigh scattering, pair creation and photo absorption. Since Compton scattering is the

dominant process between 150 keV and 10 MeV, all current tracking algorithms are based on the properties of this interaction process.

How closely the interaction points follow the Compton scattering formula

$$E'_\gamma = \frac{0.511}{1 + \frac{0.511}{E_\gamma} - \cos(\theta)} \quad (23)$$

is evaluated by the Figure of Merit (FOM)

$$FOM = \sum_i \frac{\sqrt{(\theta_i^{theo} - \theta_i^{obs})^2}}{n_i - 1}; n_i > 1 \quad (24)$$

where θ_i^{obs} are the observed scattering angles and θ_i^{theo} are the angles (in radians) from the Compton scattering formula, based on the energy deposited, $E_\gamma - E'_\gamma$, at the interaction points and n_i is the number of interaction points. If the angle θ becomes unphysical, based on the scattering energy, a penalty in the FOM sum, Eq. 24, is added. For photons with more than one interaction point, typically upper limits on the FOM for a γ ray to be considered "good" are in the range from zero up to $0.6 < FOM_{max} < 0.8$. Gamma rays that have been assigned higher FOM by the tracking algorithm are rejected. An interaction point that is not clustered with other ones (i.e., when $n_i \equiv 1$) is referred to as a *single-interaction point* γ ray. Such photons cannot be tracked and are assigned a FOM of zero, unless they are located beyond their range in the crystals, in which case they are assigned a FOM value of 1.85 (see Appendix B).

With a calibrated ^{60}Co source, the number of 1333-keV γ rays absorbed in the tracking array should be $S\epsilon_p(1333)$ (see eqs. 1–5). Thus if, in the tracked spectrum, $A_T(1333)$ counts are measured instead, the tracking efficiency for a given FOM cut is:

$$\epsilon_{track} = \frac{A_T(1333)}{S\epsilon_p(1333)} \quad (25)$$

If an uncalibrated ^{60}Co source is used, this ratio can still be found using Eq. 16 as

$$\epsilon_{track} = \frac{A_T(1333)}{\frac{A_{ext}^{obs}(1333)}{(1 - C_k(1173))(1 - C_R)(1 - C_s)}} \equiv \frac{A_T(1333)}{A^{true}(1333)} \quad (26)$$

where $A^{true}(1333)$ is the true counts in the CCcal spectrum defined in Eq. 16. For tracked data, the experimental photopeak efficiency is the array efficiency, eqs. 13 and 14, multiplied by this tracking efficiency. These are the efficiencies that we obtain below and that we present in Fig. 6.

For tracked spectra, the area of the 2506-keV peak should not be included in the (P/T) ratio as it should ideally be absent since such events should have been tracked and resolved into two γ rays of 1173 and 1333 keV. Thus, we suggest that the proper (P/T) ratio to be used and reported for *tracked* spectra is simply:

$$(P/T)^{tracked} = \frac{A_T(1173) + A_T(1333)}{A_{tot}}, \quad (27)$$

where A_{tot} is the number of counts from some lower-energy limit up to just past the 2506-keV line in the tracked spectra. Any counts in the 2506-keV peak should be considered to belong to the total part, A_{tot} . In this paper, the (P/T) ratio is measured with background subtraction under the 1173-, 1333- and 2506-keV lines.

We propose that a measure of the tracking deficiency for a ^{60}Co source is

$$TrD = \frac{A_T(2506)}{A_T(1173) + A_T(1333)}, \quad (28)$$

where the areas A_T are from the tracked spectra (for a given FOM range acceptance). Tracking can, for real data, never completely remove the summed 2506 peak and, if TrD is too large, there will be artificially summed peaks in the actual tracked spectra. Getting a high tracked efficiency, (P/T) ratio and yet a small tracking deficiency requires compromises in the values of the tracking parameters as will be discussed in the following. For a ^{60}Co source, the tracking deficiency as a function of FOM cuts has been found to be small (less than 1 % for the size of the tracking array examined in this work). The concept of the tracking deficiency can be generalized for any source as:

$$TrD = \frac{\sum_i \sum_j A_T(E_i + E_j) + \sum_i \sum_j \sum_k A_T(E_i + E_j + E_k) \dots}{\sum_i A_T(E_i)}, \quad (29)$$

where the sum is over peak areas of γ rays in coincidence and where $i < j < k$.

3.2. The clustering angle (α)

One of the most critical parameters in tracking algorithms is the clustering angle used to associate a set of interaction points with (potential) γ rays. The γ rays reconstructed in this manner may later be re-clustered (split and combined) depending on their FOM values. Even though the tracking algorithm has the ability to split and combine clusters, the initial clustering angle that is used has a strong influence on the quality of tracked spectra.

The minimum clustering angle required for good tracking can be estimated by examining the spread of angles between interaction points for a ^{60}Co source in the tracking array, as shown in Fig. 1. This curve reveals the minimum clustering angle to be used if a given probability for collecting all the interaction points for the γ rays emitted by a ^{60}Co source is to be reached.

Figure 2, which is an integral of the curve in Fig. 1, suggests that the clustering angle should be no less than around $11^\circ - 12^\circ$ in order to collect at least 90% of the interaction points created in the detectors for a ^{60}Co source. Although it is tempting to increase the clustering angle to achieve increasingly better tracked spectra, this cannot be done for in-beam data with high γ -ray multiplicity, as this would result in the mistaken clustering of separate γ rays. The probability for at least two γ rays

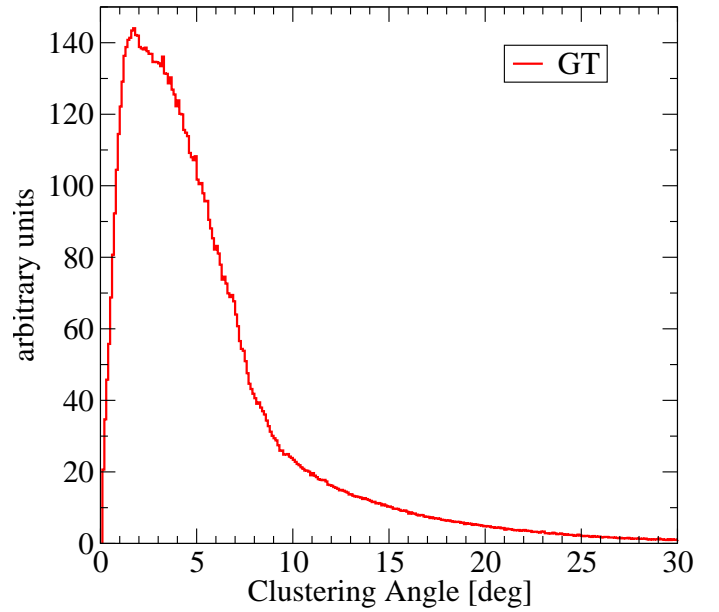


Figure 1: The measured angle spread of interaction points for the γ rays from a ^{60}Co source in the GRETINA tracking array based on the decomposed (pulse shape analyzed) data from the spectrometer.

in a cascade to be wrongly “double-clustered”, P_{dc} , is approximately:

$$P_{dc} \approx \epsilon_T \left(1 - \prod_{i=1}^{m-1} \left(1 - \frac{i\epsilon_T}{n} \right) \right) \quad (30)$$

$$n = \frac{2}{(1 - \cos(\alpha/2))} \quad (31)$$

where α is the clustering angle, ϵ_T the total array efficiency and m is the multiplicity of the γ -ray cascade from a source or from in-beam reaction residues; n is the number of clusters for the clustering angle α ¹. If one wants to keep this double-clustering probability below 1%, 5% or 10%, for a given clustering angle and calculated for the full GRETA array with 120 crystals, the maximum γ -ray multiplicity, m , that can be accepted is given in Table 2. Thus, for typical heavy-ion induced fusion reactions producing high multiplicity γ -ray cascades, the choice of clustering angle is a compromise between tracking widely-scattered γ rays and reducing the number of false double clusters.

The above discussion provides some guidance as to the value of the clustering angle to use for a given data set. One could try to optimize the α angle by maximizing at the product $[P \times P/B]$ for a representative line in the spectra. Here, P is the area of the peak and B is the background level under the same peak. This measure optimizes both the efficiency and the (P/T) ratio of the tracked spectra, thus finding the best compromise for the clustering angle.

¹If $\epsilon_T=1$ and $\alpha=12^\circ$ ($n = 365$), eqs. 30 and 31 solve the well known ‘birthday problem’; i.e., how many people have to be in a room before there is a 50% chance that two have the same birthday.

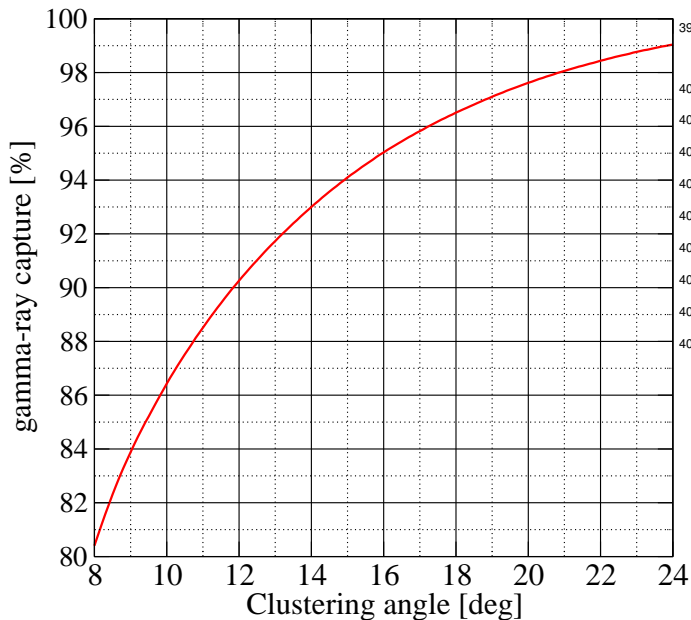


Figure 2: The minimum clustering angle needed to group interaction points into a γ ray for GRETINA with the resulting clustering efficiency given on the y axis. These curves are obtained by a simple integration of the curve displayed in Fig. 1.

4. Results and comparisons

As mentioned in the introduction, a suitable approach to test the formulas and procedures discussed above is to first apply these to data from Gammasphere. The results are presented in section 4.1. The array efficiency is extracted for GRETINA in section 4.2. Sec. 4.4 presents tracking angular correlation results while Sec. 4.5 compares the ^{60}Co spectra obtained in the Gammasphere and GRETINA arrays. Finally, Sec. 4.6 compares the (P/T) versus efficiency data for the arrays.

Table 2: The maximum multiplicity, m , that can be accepted for a given clustering angle, α , in order to keep the double clustering probability, P_{dc} , in the full GRETINA array below the limits of 1, 5 or 10% for a ^{60}Co source. For GRETINA, the photopeak efficiency has been extrapolated to be 34% (see Sec. 4.2) and a (P/T) ratio of the order of 0.6 is expected. Thus, the total array efficiency (see Eq. 30), is expected to be about 62%, the value used to produce this table.

P_{dc} \ α [deg]	<1%	<5%	<10%
8	7	15	22
10	5	12	17
12	4	10	14
14	4	8	12
16	3	7	11
18	3	7	10
20	3	6	9

4.1. The efficiency of Gammasphere

Table 3 presents measurements of the efficiency for Gammasphere. Two calibrated ^{60}Co sources were used, one isotopically pure and one mixed. The mixed-isotope source was weak and calibrated, containing ^{60}Co , ^{137}Cs and small traces of other radioisotopes. With these data, a good test of the random correction terms in the efficiency formulas is possible. With two sources, two methods and both the CCsum and CCcal spectra, there are eight measurements and the results are compared in Table 3.

Table 3: Measured array efficiencies for Gammasphere, scaled to 100 detectors, using two methods, two spectra and two sources. Traditionally, the (P/T) value derived from the CCsum spectrum is reported as the ratio for the Gammasphere array because it is the relevant ratio for spectra where gates are placed on γ rays. The deadtimes used in the CSM analysis are discussed in Appendix A.1.

	SPM	CSM
CCsum spectrum, $C_s=0.040(5)$		
$\epsilon_P(\text{mixed})$	8.6(9)%	8.0(3)%
$\epsilon_P(\text{pure})$	8.8(2)%	7.6(8)%
$(P/T)^{\text{obs}}$	0.471(5)	0.471(5)
$(P/T)^{\text{true}}$	0.514(5)	0.492(5)
C_o	1.10(5)	1.10(5)
CCcal spectrum, $C_s=0$		
$\epsilon_P(\text{mixed})$	7.9(2)%	8.3(3)%
$\epsilon_P(\text{pure})$	7.9(2)%	7.8(4)%
$(P/T)^{\text{obs}}$	0.460(5)	0.460(5)
$(P/T)^{\text{true}}$	0.537(5)	0.540(5)
C_o	1.10(5)	1.10(5)

For the CSM method, in calculating the live fraction L_F (see Eq. 8) for Gammasphere, we take into account various dead-times of the system as well as other inefficiencies of the DAQ readout system, see Appendix A.1. Using all the methods and sources, with proper corrections, the efficiency of Gammasphere is determined to be 8.2(1)% with a (P/T) ratio of 0.52 using the weighted sum of all the results. The (P/T) ratio and efficiency are somewhat lower than those reported in Ref. [30] because the light collection efficiency in the BGO Compton Suppressors has deteriorated somewhat over time. In 2007, the efficiency of Gammasphere was measured to be 8.9(1) with a (P/T) ratio of 0.54, using slightly less accurate formulas compared to those presented in this work. For the comparison with the GRETINA tracking array, the 2007 optimal Gammasphere performance regarding the (P/T) will be used as the standard.

4.2. The efficiency of GRETINA at ANL

At the time of these measurements, GRETINA consisted of 28 crystals. The array efficiency at 1333 keV was measured with two sources, as was the case with Gammasphere (see Sec. 4.1). The clustering angle for tracking was set to 20° . The results are presented in Table 4. As discussed in Sec. 3, the tracking efficiency is obtained by comparing the number of counts in the photopeaks of the tracked spectrum with the corrected counts

432 from Eq. 16. The tracking efficiency is given for tracked spectra
 433 without FOM cuts. The subscripts *wsi* and *nsi* refer to spectra
 434 that include and exclude single interactions in the tracking, re-
 435 spectively. An experimentally measured value of $C_f = 1.00645$
 436 was used (see Sec. 4.4).

Table 4: Measured array efficiencies for GRETINA with 28 crystals at the nominal distance of 18.5 cm at ANL. The deadtimes used in the CSM analysis are discussed in Appendix A.2. See text for details.

	SPM cal	CSM cal	SPM sum
$\epsilon_P(\text{mixed})$	6.02(15)%	6.24(18)%	-
$\epsilon_P(\text{pure})$	6.40(6)%	6.0(6)%	6.5(6)%
$(P/T)^{\text{obs}}$	0.321(3)	0.321(3)	0.192(2)
$(P/T)^{\text{true}}$	0.386(4)	0.382(3)	0.363(11)
$\epsilon_{\text{track},\text{nsi}}$	91(1)%	92(2)%	92(1)%
$\epsilon_{\text{track},\text{wsi}}$	93(1)%	94(2)%	93(1)%
C_s	0	0	0.293(5)
C_0	1.02(2)	1.02(2)	1.02(2)

437 The efficiency was also measured with an external detector (as
 438 described in section 2.2) to be 6.39(17)%. The errors in Table 4
 439 take into account the full error propagation for all the variables
 440 in eqs. 13 and 14 above.

441 The photopeak efficiency for GRETINA is determined to be
 442 6.45(4)%, using a weighted mean of the values in Table 4,
 443 combined with the external detector measurement, and the true
 444 (P/T) ratio is measured to be 0.38.

445 From these results, the expected efficiency of the full GRETA
 446 spectrometer can be estimated. The full 4π array will have 120
 447 crystals; the occupancy of GRETINA for the current measurement
 448 was thus $28/120=23.3\%$. The efficiency per crystal is deter-
 449 mined to be 0.229(2)%. Hence, for a 4π array, an efficiency
 450 of at least 27.4(2)% would be expected using simple scaling.
 451 This is, however, only a lower limit since the more crystals fill
 452 the array, the less ‘open’ surface there is where γ rays can es-
 453 cape and the scaling should, therefore, not be linear. Using
 454 the AGATA–GEANT4 code [32] (with an uncertainty of 10%
 455 in the simulations) for this scaling yields a 4π array photopeak
 456 efficiency of 34(4)%, or about 4 times that of Gammasphere.

4.3. The efficiency of GRETINA at MSU

458 At MSU, the GRETINA array was configured slightly more
 459 compact (see Sec. 5) and the analysis of the data from the MSU
 460 setup is presented in Table 5. A weak, calibrated ^{60}Co source
 461 was used, thus, all spectra were background subtracted.

4.4. Angular correlations in tracking arrays

463 The fact that tracking algorithms cluster together interactions
 464 within a given solid angle impacts angular correlation measure-
 465 ments from tracked data. The extent of this impact is illus-
 466 trated by extracting angular correlation information for the γ
 467 rays from a ^{60}Co source. The procedure is as follows: for each

Table 5: Measured array efficiencies for GRETINA at MSU with 28 crystals at the nominal distance of 18.5 cm from the target position. See text for details.

	SPM cal	SPM sum
$\epsilon_P(\text{pure})$	6.30(14)%	6.58(44)%
$(P/T)^{\text{obs}}$	0.366(5)	0.215(3)
$(P/T)^{\text{true}}$	0.434(5)	0.428(20)
$\epsilon_{\text{track},\text{nsi}}$	89(1)%	89(3)%
$\epsilon_{\text{track},\text{wsi}}$	92(1)%	93(3)%
C_s	0	0.316(5)
C_0	1.02(2)	1.02(2)

468 event where one 1173– and one 1333–keV γ ray are present,
 469 the angle between the first interaction points for the two pho-
 470 tons is found and is histogrammed, herewith revealing the set
 471 of *correlated* events.

472 This event is also stored and used when the next coincidence
 473 event is encountered to construct angles between *uncorrelated*
 474 first interaction points from pairs of γ rays originating from
 475 events measured at different times. The ratio of the spectrum
 476 of correlated angles to that of uncorrelated ones reveals the
 477 angular correlation and is presented in Fig. 3 for GRETINA,
 478 while using a clustering angle of 10° . Conveniently, the uncor-
 479 related spectrum also allows us to experimentally determine the
 480 C_f value discussed in Sec. 2.1. The angular correlation func-
 481 tion [29], $\omega(\theta) = 1 + 0.102041P_2(\cos\theta) + 0.00907P_4(\cos\theta)$, is
 482 simply weighted with the normalized uncorrelated spectrum.

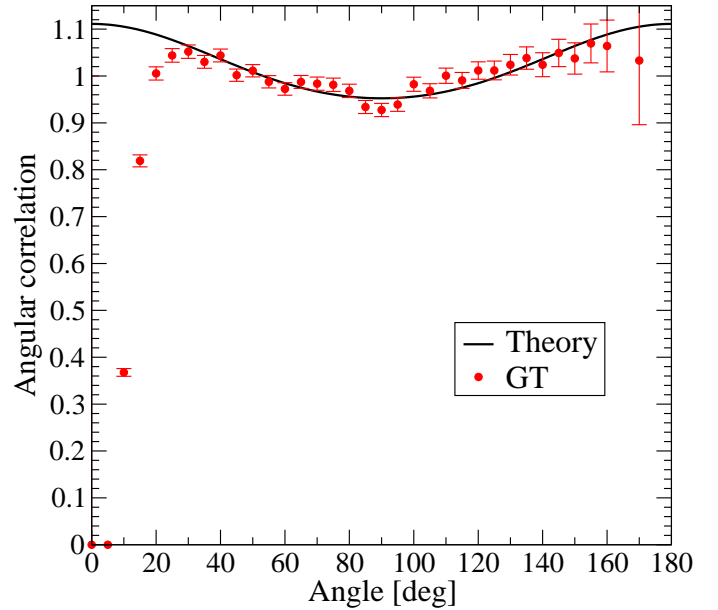


Figure 3: Angular correlation extracted from tracked GRETINA (GT) data for a ^{60}Co source using a clustering angle of 10° . For the tracking, a FOM acceptance from zero to 0.8 was used and the theoretical spectrum is shown without any attenuation. See text for details.

The drop at small angles in Fig. 3 comes from the fact that, if two γ rays are within the pre-determined clustering angle, they will (using current tracking codes) mostly be added up rather

486 than be recognized as individual photons (see the tracking de-
 487 ficiency discussion in Sec. 2.2). As can be seen in Fig. 3, the
 488 *effective* clustering angle is slightly larger than the 10° specified
 489 for the tracking because two nearby γ rays may have *some* in-
 490 teraction points that are within the clustering angle.

491 The tracking arrays offer an angular resolution of $1^\circ - 2^\circ$. If
 492 needed, the $\gamma - \gamma$ angular correlation can be extended towards
 493 lower angles using a "mix before track" method developed
 494 within the AGATA collaboration [33].

495 4.5. Comparing ^{60}Co source spectra

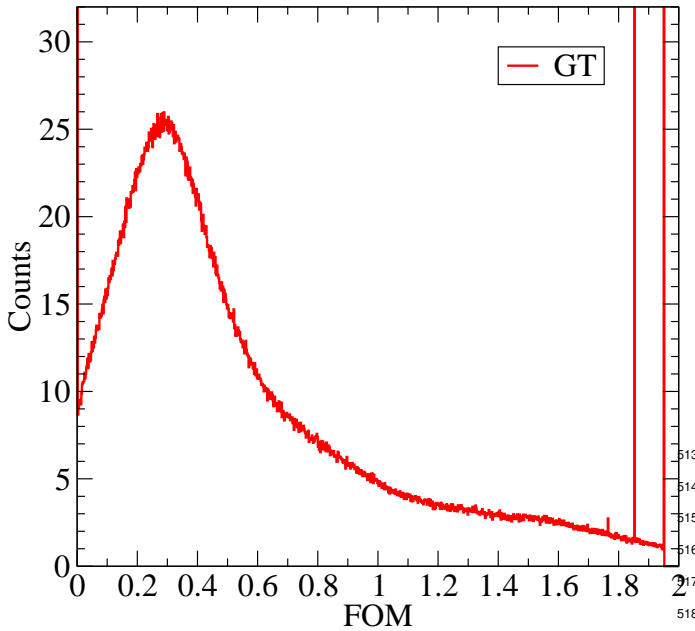


Figure 4: The FOM spectrum for GREYINA for a ^{60}Co source. The single-
 interaction point γ rays that occurred too deep in the crystals are marked with
 a FOM=1.85 rather than zero. Overflows are marked with at FOM of 2.0. See
 text for details.

496 Figure 4 provides the FOM distributions (see Sec. 3.1) for
 497 tracked γ rays obtained from the GREYINA spectrometer with
 498 a ^{60}Co source. In GREYINA, $\sim 7\%$ of the γ rays are assigned
 499 FOM=0 by the tracking algorithm and $\sim 8\%$ are single inter-
 500 actions happening too deep into the Ge crystal for this to be
 501 probable (see Appendix B). Thus, the latter events are marked
 502 with a FOM=1.85, so that they can be rejected in the ensuing
 503 sorting.

504 Figure 5 compares ^{60}Co source spectra from GREYINA at
 505 ANL, with and without including single interaction γ rays, and
 506 a spectrum from Gammasphere. A FOM cut of 0–0.64 for
 507 GREYINA was applied. This particular FOM cut was selected
 508 so that 70% of the γ rays are accepted in GREYINA (see Fig. 4).
 509 The spectra are normalized such that the same number of counts
 510 are present in the photopeaks and no background subtraction
 511 has been applied.

512 In all cases, the (P/T) ratio was determined using a low-energy

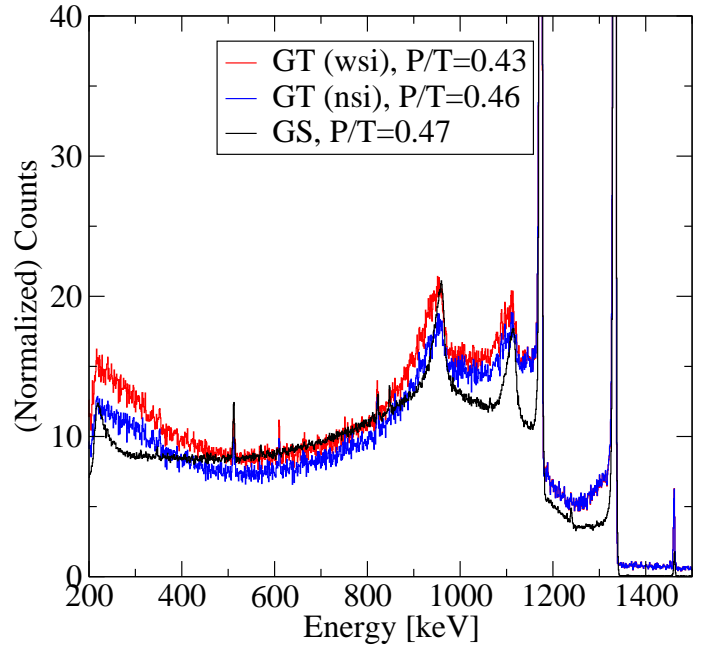


Figure 5: Comparison of spectra from ^{60}Co from GREYINA (GT), with and
 without single interactions at ANL, and Gammasphere (GS). In all cases, the
 spectra have been normalized to have the same number of counts in the photo-
 peaks.

bound of 200 keV because Gammasphere was equipped with
 Ta/Cu absorbers which affect spectra below this energy. At the
 time the data was recorded, GREYINA had Ta absorbers in front
 of the seven modules. Hence, a lower bound of 200 keV was
 applied to all the tracked spectra and provides for a fair com-
 parison of the measured (P/T) ratios.

4.6. Comparing the (P/T) ratios versus the efficiency curves for GREYINA

The (P/T) ratio vs. photopeak efficiency curves for GREYINA
 can be found in Figs. 6 and 8, for clustering angles of 20° and
 10° , respectively. The clustering angle is typically chosen be-
 tween these limits, depending on the γ -ray multiplicity (see dis-
 cussion in Sec. 3.2). The two curves in the figures demonstrate
 the effect of *including* (wsi) and *excluding* (nsi) photons with
 a single-interaction points. The curves are provided for FOM
 cuts of 0–0.2, 0.4... 2.0 (from left to right) where a FOM cut of
 0–2.0 is equivalent to no cut at all.

5. Discussion

As can be seen in Figs. 6–8, in GREYINA there is not much
 difference between the nsi and wsi curves in terms of efficiency
 (see also Table 4). Indeed, when extracting the probability for
 a photopeak event as a function of the number of interaction
 points, after tracking, it is clear that there are many single-
 interaction points that do not contribute to the photopeaks for

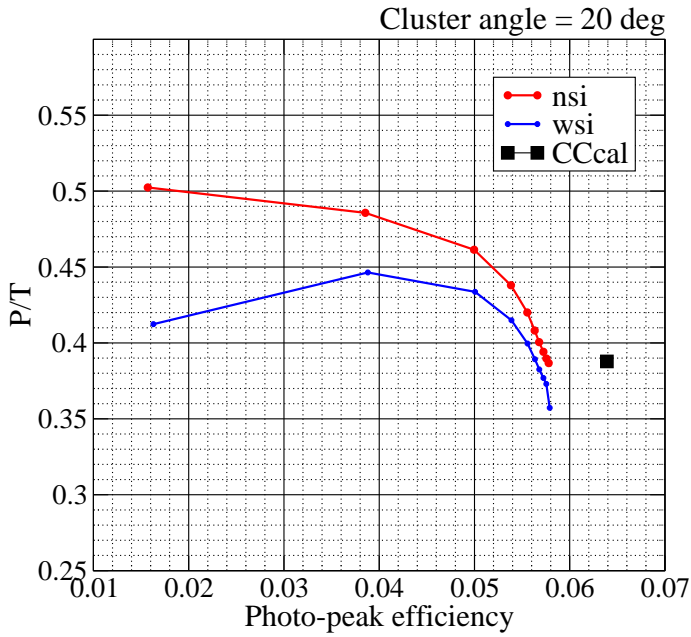


Figure 6: The (P/T) ratio vs. photopeak efficiency curves for GREINA (ANL setup), with 7 closed-packed modules, when a clustering angle of 20° is used. The lower curve includes single interactions (wsi) and the upper curve is obtained without these interactions (nsi).

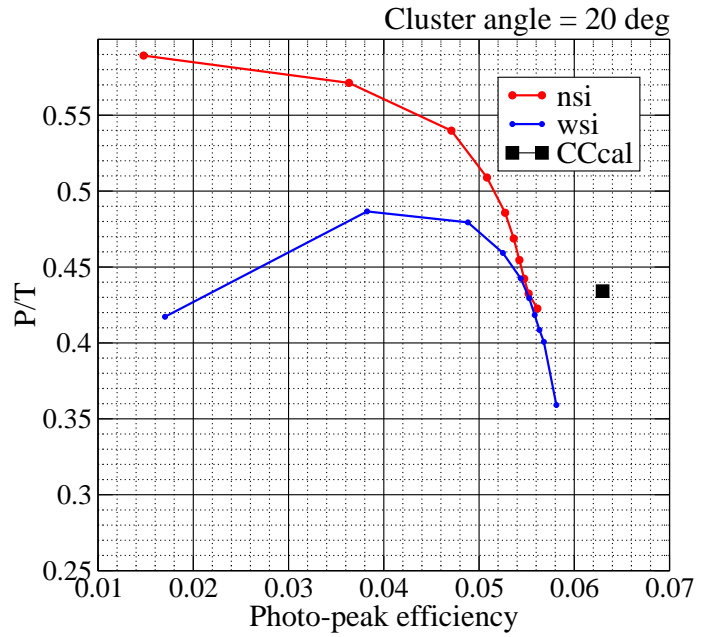


Figure 7: The (P/T) ratio vs. photopeak efficiency curves for GREINA (MSU setup), with 7 closed-packed modules, when a clustering angle of 20° is used. The lower curve includes single interactions (wsi) and the upper curve is obtained without these interactions (nsi).

537 a ^{60}Co source: this is shown in Table 6. Only 2% of the pho-
 538 topeaks contain single interactions. Data from GEANT4 simu-
 539 lations suggest that $\sim 10\%$ of the photopeaks ought to be from
 540 single-interaction events. The data from the GEANT4 simu-
 541 lations were smeared to have the same position and energy un-
 542 certainty as data from the tracking array [7, 34] and a packing
 543 parameter of 6 mm was used (*i.e.*, GEANT4 interactions within
 544 6 mm were combined into one interaction). It was not possible
 545 to find realistic packing parameters that could fully reproduce
 546 the data in Table 6.

Table 6: Distribution of the number of interaction points in the tracked *photo-*
peak γ rays for a ^{60}Co source in GREINA and those obtained from a GEANT4
 simulation with the parameters outlined in the text.

number of interaction points	GREINA photopeak	GEANT4 photopeak
1	2%	10%
2	21%	27%
3	35%	31%
4	24%	21%
5	13%	10%
6	4%	3%
7	1%	1%

547 In the GREINA decomposition, the fits of the segment
 548 traces [14] allow for more than one interaction per segment.
 549 One might suspect that the fitting function sometimes places
 550 two interaction points in a segment where there should have
 551 been only one – because it results in a better χ^2 in the fitting
 552 procedure. Hence, it is possible that, in general, the GREINA

decomposition overestimates the number of interaction points associated with a photon.

Both the array efficiency and, especially, the tracking efficiency depend on the degree to which a tracking array is compact, *i.e.*, how closely the crystals are packed in the array. A measure of the compactness of a tracking array may be obtained as follows: for each crystal, one can count how many of the sides of the crystal have a near (contact) neighbor, add up the numbers for the individual crystals and divide by the number of crystals times six (*i.e.*, the total number of sides). With 28 crystals during the campaign at ANL, a compactness value of 63% is obtained (see section 4.2). In an earlier setup at MSU, a compactness of 70% was achieved (see section 4.3). The detailed effect of compactness on the tracking performance is under investigation [35].

Figure 9 presents the absolute efficiency for Gammasphere and GREINA as a function of γ -ray energy. The GREINA data were tracked with a clustering angle of 20° and a FOM cut of 0–0.8. It was possible to determine the efficiency only up to ~ 3 MeV because of the energy range selected for the central contact during the measurements. The Gammasphere curve is given for the standard 100 detectors, as well as when scaled to the same occupancy as GREINA; *i.e.*, 28/120.

Finally, using a ^{60}Co source, we suggest that it is possible to numerically compare Gammasphere and GREINA by evaluating a figure of merit defined as $[\epsilon_p \times (P/T)]$, and using the optimum place on the (P/T) ratio vs photopeak efficiency curves presented in Figs. 6–8. Using spectra from the GREINA tracking

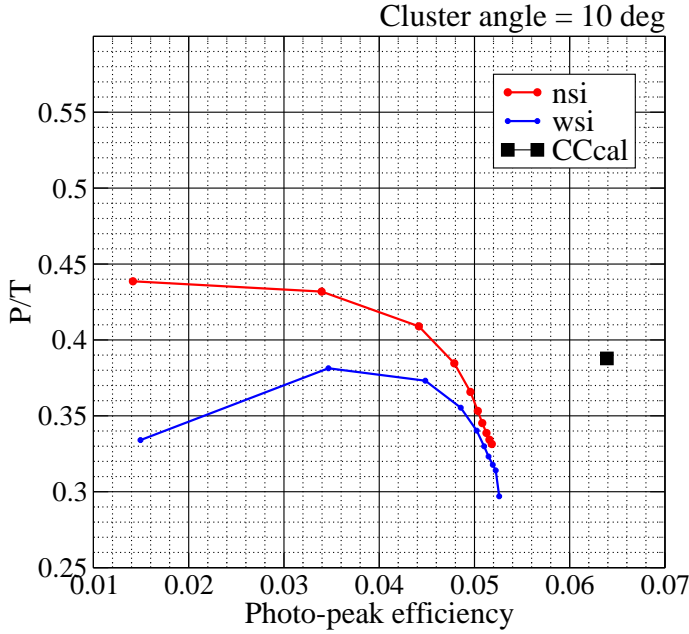


Figure 8: Same as Fig. 6, but now using a clustering angle of 10° .

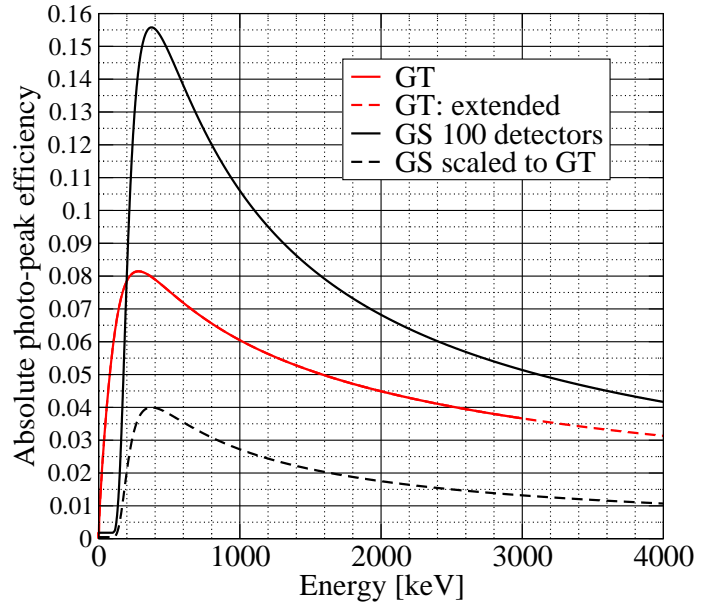


Figure 9: The absolute efficiency of Gammasphere and GRETINA (with 28 crystals) as a function of energy.

array with a clustering angle of 20° , and excluding (or including) the single-interaction points, the results are given in the second (third) column of Table 7.

If one takes $[\epsilon_p \times (P/T)]$ as the measure, with 100 modules in Gammasphere and 28 crystals in GRETINA, Gammasphere is about twice as sensitive as GRETINA. However, when scaled to an occupancy of 23.3% (*i.e.*, that of GRETINA), GRETINA is approximately twice as sensitive as Gammasphere (see Table 8). If a figure of merit of $[\epsilon \times (P/T)]^2$ was used (Table 7), which would be more relevant for gated coincidence spectra [23], GRETINA would be about four times as sensitive as Gammasphere. The $[\epsilon_p \times (P/T)]$ figure of merit used here is, of course, only one of many possible measures. In many in-beam experiments, the superior angular resolution and, thus, Doppler correction offered by the tracking arrays will be of much more importance [36].

Table 7: Numerical comparison of Gammasphere and GRETINA using the figure of merit measure of $[\epsilon_p \times (P/T)]$, including single-interaction γ rays (wsi) and excluding them (nsi). See text for details.

device	$[\epsilon_p \times (P/T)]$	
	(nsi)	(wsi)
Gammasphere	0.0427	0.0427
GRETINA	0.0236	0.0223

6. Conclusions and outlook

We have found that, generally speaking, tracking γ detector arrays are more challenging to characterize than the Compton-suppressed γ -ray spectrometers of the previous generation.

Table 8: Comparison of Gammasphere and GRETINA using the figure of merit measures of $[\epsilon_p \times (P/T)]$ and $[\epsilon_p \times (P/T)]^2$, and where Gammasphere data have been scaled to have the same occupancy as GRETINA. The (nsi) results exclude single interactions and the (wsi) results include them. See text for details.

device	$[\epsilon_p \times (P/T)]$		$[\epsilon_p \times (P/T)]^2$	
	s(nsi)	s(wsi)	s(nsi)	s(wsi)
Gammasphere	0.0110	0.0110	$1.21 \cdot 10^{-4}$	$1.21 \cdot 10^{-4}$
GRETINA	0.0236	0.0223	$5.57 \cdot 10^{-4}$	$4.97 \cdot 10^{-4}$

However, based on current extrapolations to a full 4π array, they will provide superior performance mainly due to the large HPGc coverage while maintaining a good (P/T) ratio. Possible improvements in electronics, signal-decomposition and tracking algorithms could translate into a better (P/T) ratio and further enhance their potential.

In this work, an attempt was made to provide a formalism to determine the array photopeak efficiencies, tracking efficiencies and true peak-to-total ratios. Some guidelines regarding clustering angles to be used in the γ -ray tracking algorithm have also been proposed.

Throughout this work, a ^{60}Co source was used to characterize the arrays. Many optimizations of the tracking parameters will remove low-energy γ rays in the ^{60}Co spectra and, thus, appear to improve the peak-to-total ratio. However, further analysis often reveals that the photopeaks associated with low energies are much reduced as well. We suggest that a ^{166}Ho source is a better choice to use for the characterization of tracked spectra. This source has transitions that are in coincidence with each other and this will allow to improve the tracking algorithms and optimize their parameters. In addition, it has low-energy lines that a ^{60}Co source lacks and it has a strong branch with four γ

rays in coincidence with respective energies of: 711.7, 810.3, 184.4 and 80.6 keV. Other γ rays in coincidence can be used as well. Work is in progress on improving the tracking of data from the GRETINA spectrometer using this source [37].

We have developed software that can translate AGATA data into data in the GRETINA data format (*i.e.*, data containing the interaction point coordinates, energies and timestamps of the γ -ray interactions in the crystals). This would allow for a direct comparison of the performance of the two tracking arrays. Unfortunately, results of an analysis of AGATA data will be published elsewhere [38].

7. Acknowledgments

This material is based upon work supported by the U.S. Department of Energy, Office of Science, Office of Nuclear Physics, under contract number DE-AC02-06CH11357. This research used resources of the ANL's ATLAS facility, which is a DOE Office of Science User Facility. LBNL is supported by the U.S. Department of Energy under Contract No. DE-AC02-05CH11231 and L. Riley acknowledges support from NSF through grant no. PHY-1303480. This work was also supported by the French National Center of Research, CNRS. D. R. was partially supported by the P2IO Excellence Laboratory. We acknowledge valuable discussions with J. Ljunvall and A. Lopez-Martens.

Appendix A. Deadtime and random rates

If calibrated sources are used to determine the efficiencies of the spectrometers, the deadtimes of the DAQ systems need to be determined. This, of course, also holds if the array is used to determine absolute cross sections.

Appendix A.1. Dettimes in Gammasphere

In the analog Gammasphere data acquisition system (DAQ), there are two deadtimes. The first is in the pre-trigger circuitry and is about 1-2 μ s. The second deadtime is in the readout system and is about 19-21 μ s depending on the setup. The total DAQ live fraction is taken to be the product of the resulting live fractions. The fact that the analog DAQ stops, for the order of a minute, every time the analog Gammasphere event builder is reset must also be taken into account, herewith resulting in an additional deadtime. This deadtime can be found by inspection of the rate spectra.

The formulas of Ref. [24] were used to calculate the live fractions. The rates in Gammasphere for the the mixed and pure sources were 1.47- and 11.0 kHz, respectively and the live fractions were found to be 0.967 and 0.711, see Table 3. The C_R values for the mixed source are determined to be $26(6)10^{-6}$ and $31(7)10^{-8}$ for the CCcal and CCsum spectra, respectively. For the pure source a value of zero was used.

Appendix A.2. Dettimes in tracking arrays

Both GRETINA and digital Gammasphere (DGS) have DAQ systems that, as opposed to the analog Gammasphere DAQ system, only have channel deadtimes. Thus, unlike analog Gammasphere, the DAQs for GRETINA and DGS are never totally blocked at any given time, but the overall efficiency is, however, reduced by the unavailability of the channels that are busy (*i.e.*, dead). Using the CSM with the CCcal spectrum, it is mathematically possible to take this into account in Eq. 8, through the L_F factor – even though, in this case, L_F reflects a reduction in efficiency rather than a traditional live fraction of the DAQ. For the CCcal spectrum, the channel live fraction is also the overall array live fraction. However, for the CCsum as well as tracked spectra, the overall array live fraction will be different and will depend on, among other things, the γ -ray multiplicity.

The rate in GRETINA was 3.49 kHz when the weak mixed source was placed at the target position. The channel deadtime was measured to be 22 μ s. To be able to handle the rate in GRETINA caused by the 'pure' source, the DAQ was pulsed on and off with an on fraction of 8.92(8)%. The average rate was observed to be 445 Hz, so the actual rate, while the GRETINA DAQ was on, was therefore 5.00 kHz. It follows that the per-crystal counting rates for the two sources were 125 Hz and 179 Hz, resulting in effective live fractions of 0.997 and 0.996, respectively, for the mixed and 'pure' source. Thus, for both sources, the effect of deadtime is negligible. The random rates for the mixed source resulted in $C_R = 25(5)10^{-6}$ and $89(17)10^{-8}$ for the CCcal and CCsum spectra, respectively. For the pure source the C_R value was set to zero.

Appendix B. Range of γ rays in Ge

Photons penetrating a Ge crystal are absorbed with a probability of

$$p(z) = 1 - e^{-(\mu/\rho)\rho z} \quad (\text{B.1})$$

where z is the depth in the crystal from the front face, ρ the density of Ge and (μ/ρ) the mass attenuation coefficient for Ge which depends on the energy of the photon and are tabulated in Ref. [39]. One can, for a given energy of a γ ray, determine the depth in the crystal, $z_{85\%}$, where the γ ray has been fully absorbed with a 85% probability. Fig. B.10 shows the $z_{85\%}$ range values for energies relevant for γ -ray spectroscopy. These range values are used in the tracking procedure to mark (with a FOM of 1.85) single-interaction γ rays that have less than a 15% probability for having interacted at the z range determined by the decomposition and tracking algorithms.

References

- [1] P. J. Nolan, F. A. Beck, and D. B. Fossan, *Annu. Rev. Nucl. Sci.*, 45 (1994) 561.
- [2] J. Eberth and J. Simpson, *Progress in Particle and Nuclear Physics*, 60 (2008) 283.

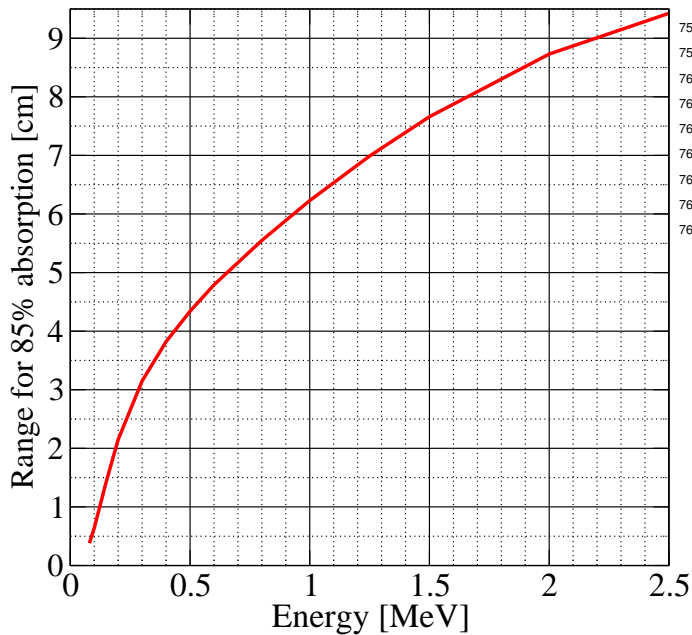


Figure B.10: The depth in a Ge crystal at which a γ ray has been absorbed with a 85% probability. See text for details.

[32] E. Farnea, Nucl. Instr. Meth. A, 621 (2011) 331 – 342.
 [33] J. Ljungvall et al., to be published.
 [34] P. Soderstrom, et al., Nucl. Instr. Meth. A, 638 (2011) 96 – 109.
 [35] J. Dudouet, to be published.
 [36] J. Gerl et al., to be published, (2016).
 [37] T. Lauritsen and A. Korichi *et al.*, to be published.
 [38] A. Korichi et al., in preparation.
 [39] URL <http://physics.nist.gov/PhysRefData/XrayMassCoef/chap2.html>.

[3] I. Y. Lee, M. A. Deleplanque, and K. Vetter, Rep. Prog. Phys., 66 (2003) 1095.
 [4] M. A. Deleplanque, et al., Nucl.Instrum.Methods Phys.Res., A430 (1999) 292.
 [5] J. van der Marel and B. Cederwall, Nucl. Instr. Meth. A, 437 (1999) 538 – 551.
 [6] G. J. Schmid, et al., Nucl. Instr. Meth. A, 430 (1999) 69 – 83.
 [7] D. Bazzacco, Development of gamma-ray tracking detectors, EU TMR network project, unpublished code.
 [8] A. Lopez-Martens, et al., Nucl. Instr. Meth. A, 533 (2004) 454 – 466.
 [9] F. Didierjean, G. Duchêne, and A. Lopez-Martens, Nucl. Instr. Meth. A, 615 (2010) 188 – 200.
 [10] J. Simpson, Z. Phys., A358 (1997) 139.
 [11] I-Y. Lee, Nucl. Phys., A520 (1990) 641c.
 [12] R. Janssens and F. Stephens, Nucl. Phys. News Int., 6 (1996) 9.
 [13] S. Akkoyun, et al., Nucl. Instr. Meth. A, 668 (2012) 26 – 58.
 [14] S. Paschalis, et al., Nucl. Instr. Meth. A, 709 (2013) 44 – 55.
 [15] I-Yang Lee and J. Simpson, Nuclear Physics News, 20 (2010) 23.
 [16] S. Galès, Nucl. Phys., A834 (2010) 717c.
 [17] A. Andrichetto, et al., Nucl. Phys., A834 (2010) 754c.
 [18] URL <http://www.ganil-spiral2.eu/>.
 [19] H. H. Gutbord, Nucl. Phys., A752 (2005) 457.
 [20] G. Savard, et al., Hyperfine Interactions, 199 (2011) 301–309.
 [21] URL <http://www.nscf.msu.edu/>.
 [22] E. S. Reich, Nature, 477 (2010) 15.
 [23] D. C. Radford, Proceedings of the International Seminar on the Frontier of Nuclear Spectroscopy, Kyoto, Japan, World Scientific (1992).
 [24] G. F. Knoll, Radiation Detection and Measurement, New York : Wiley (2000).
 [25] G.A. Brinkman and A.H.W. Aten and J. Veenboer, Appl. Rad. Isot, 14 (1963) 153.
 [26] J.M.R Hutchinson and W.B. Mann and P.A. Mullen, NIM, 112 (1973) 187–196.
 [27] I.J. Kim and C.S. Park and H.D. Choi, Appl. Rad. Isot, 58 (2003) 227–233.
 [28] T. Vidmar, et al., Appl. Rad. Isot, 67 (2009) 160.
 [29] K. Siegbahn, Alpha-, Beta- and Gamma-ray Spectroscopy, North Holland (1965).
 [30] T. Lauritsen, et al., Phys.Rev. C, 75 (2007) 064309.
 [31] G. Duchene, et al., Nucl. Instr. Meth. A, 432 (1999) 90–110.